BAND DIAGRAMS FOR WEBS
DRAFT - NOT FOR DISTRIBITION

HEATHER M. RUSSELL (UNIVERSITY OF RICHMOND) AND JULIANNA S. TYMOCZKO (SMITH COLLEGE)

1. Fodder for an introduction

$\mathfrak{sl}_n$ webs are certain plane graphs that act as the morphisms in a diagrammatic category encoding the representation theory of $U_q(\mathfrak{sl}_n)$. We are interested in exploring the combinatorics of the web basis as it relates to topology and representation theory. Motivated by work of Francis Fung and conjectures of Mikhail Khovanov, our first project constructed a basis for the (co)homology of certain Springer varieties indexed by marked webs which arise in categorified knot invariant theory. Springer varieties are especially interesting because of the Springer correspondence which provides a geometric construction of all irreducible representations of Weyl groups... (smart words here). This led to a study of the symmetric group action on webs. (Pieces of this have also been done by Stroppel and her coauthors and Rhoades and his coauthors.)

Webs are naturally endowed with a symmetric group action coming from "flattening" the knot theoretic braiding – meaning we specialize the quantum parameter q. Our work and work of others shows that this action on $\mathfrak{sl}_2$ and $\mathfrak{sl}_3$ webs is irreducible and corresponds to two-row and three-row rectangular partitions, respectively. The $n = 2$ case is well-understood and aligns with many other well-known bases. The $n = 3$ case is interesting. All existing results about the web basis are more-or-less negative in the sense that the $\mathfrak{sl}_3$ web basis does not align with any other well-known bases for representations of either the symmetric group or quantum groups. After $n = 3$, there is not a canonical choice of basis webs, though there still may be something to say there eventually.

Webs are naturally indexed by tableaux (Westbury, Khovanov, Kuperberg, Tymoczko, Fontaine, wave diagrams and L-Tris paper). Another well-known basis for symmetric group representations indexed by tableaux is Young's natural basis or the Specht basis. We noted early on that these bases are not the same meaning the bijection between webs and tableaux does not induce an S_n-equivariant map from web space to the Specht module. The question became - to what extent are these bases related?

In our previous paper on $\mathfrak{sl}_2$ webs, we showed that the change of basis matrix between these representation spaces (when both bases are equipped with the partial order on webs) is unitriangular with additional vanishing entries. We conjecture the same to be true for $\mathfrak{sl}_3$ webs. In the process of working to prove this result, we developed a combinatorial object we call a *bands diagram*. This object is sort of an intermediary between webs and tableaux. The purpose of this paper is to investigate combinatorial properties of bands diagrams. The main application of this work is to hopefully settle our conjecture about the relationship between the Specht and web bases in the $\mathfrak{sl}_3$ setting.

MOVED FROM WEBS... One can further endow the space of webs with braiding morphisms. Using these, the diagram of any braid or link can be interpreted as a map between representations of quantum groups. In fact, the resulting maps are invariant under the framed Reidemeister moves and form a family of so-called quantum link and tangle invariants including the celebrated Jones polynomial.

Our motivation for investigating an additional structure on webs comes from representation theory. Specializing the parameter q to an appropriate constant ($\pm$ 1 depending on choice of web relations and braiding morphism), one can "flatten" the braiding morphism and construct a symmetric group action on bottom webs. We and others have explicitly shown this action on certain subspaces of bottom webs in the $k = 2, 3$ case is irreducible and have identified which symmetric group representations arise [**?**, **?**, **?**]. While we have not worked it out, experts assure us that an appropriate invocation of Schur-Weyl duality implies irreducibility for all k. Our ongoing work studies the space of bottom webs, specifically comparing the web and Specht bases of symmetric group representations.

Date: Fall 2019.

2. Webs and Tableaux

Given $k \geq 2$, an $\mathfrak{sl}_k$ web is a plane graph that act as a morphism in a diagrammatic category encoding the representation theory of $U_q(\mathfrak{sl}_k)$. Webs are drawn in a rectangular region with boundary vertices on the top and bottom edges of the region. All boundary vertices are univalent, and all internal vertices are trivalent. The edges carry labels that depend on the value of k.

Each web encodes a unique intertwining map between representations of $U_q(\mathfrak{sl}_k)$. The bottom and top boundary vertices of a web indicate the domain and codomain. The internal structure and labels of a web encode the map itself. There are diagrammatic relations between (linear combinations of) webs that represent the same map. See [**?**, **?**, **?**] for more on webs and their connection to quantum representation theory.

Precise labeling conventions and relations for webs differ slightly across the literature. We use those found in Kuperberg's work [**?**, **?**] though Kuperberg typically draws webs with boundary on a disk with a basepoint rather than along a horizontal axis.

In this section, we define $\mathfrak{sl}_2$ webs, $\mathfrak{sl}_3$ webs, and standard Young tableaux and describe combinatorial bijections between certain subsets of these objects. These bijections are key in understanding the relationship between the Specht and web bases for symmetric group representations.

2.1. $\mathfrak{sl}_2$ and $\mathfrak{sl}_3$ Webs.

$\mathfrak{sl}_2$ webs – also known as Temperley-Lieb diagrams – are ubiquitous in mathematics and extensively studied. Our main motivation in including them in this paper is to contrast their structure and properties with those of $\mathfrak{sl}_3$ webs.

Definition 2.1. An $\mathfrak{sl}_2$ *web* on $n+m$ points is a crossingless matching in a rectangular region pairing n points on the bottom and m points on top possibly with circles in the interior. An $\mathfrak{sl}_2$ *bottom web* is an $\mathfrak{sl}_2$ web on $2n+0$ points for some $n \in \mathbb{N}$.

Let $\mathcal{W}$ be the set of all $\mathfrak{sl}_2$ webs with a fixed number of top and bottom boundary points. Denote by $\Gamma^{\mathcal{W}}$ the space of $\mathbb{C}[q,q^{-1}]$- linear combinations of webs in $\mathcal{W}$ modulo the relation that a web with a circle component is equal to the result of removing the circle and multiplying by a factor of $-q-q^{-1}$. See Figure 1 for an example of an $\mathfrak{sl}_2$ bottom web with this relation applied. We will call an $\mathfrak{sl}_2$ web *reduced* if it has no circle components. The reduced webs in $\mathcal{W}$ form a basis for $\Gamma^{\mathcal{W}}$.

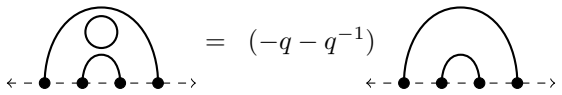

Figure 1. Removing a circle from an $\mathfrak{sl}_2$ web

Definition 2.2. An $\mathfrak{sl}_3$ *web* is an oriented, plane graph in a rectangular region with boundary vertices on the top and bottom edges of the region such that: all boundary vertices are univalent, all internal vertices are trivalent, and every vertex is a source or sink. As with $\mathfrak{sl}_2$ webs, an $\mathfrak{sl}_3$ web can have disconnected oriented circle components in the interior of the region. An $\mathfrak{sl}_3$ *bottom web* is an $\mathfrak{sl}_3$ web with no endpoints on the top boundary of the rectangular region.

Let $\mathcal{W}$ be the set of all $\mathfrak{sl}_3$ webs with a fixed set of boundary vertices and boundary orientations. Denote by $\Gamma^{\mathcal{W}}$ the space of $\mathbb{C}[q,q^{-1}]$-linear combinations of webs in $\mathcal{W}$ equipped with the relations shown in Figure 2. A web is called *reduced (or non-elliptic)* $\mathfrak{sl}_3$ if it has no circle components and no closed square or bigon faces. Using the $\mathfrak{sl}_3$ web relations, every web can be expressed uniquely as a linear combination of non-elliptic webs. An example is shown in Figure 3. The reduced webs in $\mathcal{W}$ form a basis for $\Gamma^{\mathcal{W}}$.

In this paper, we will focus exclusively on bottom webs. To track combinatorial statistics for these webs, we enumerate their vertices from left to right beginning with 1. Let $\mathcal{W}_{2n}$ be the set of $\mathfrak{sl}_2$ webs on $2n+0$ points, and let $\mathcal{W}_{3n}$ be the set of $\mathfrak{sl}_3$ webs with 0 top boundary points and $3n$ bottom boundary points all of which are sources. Further, we will specialize to $q=1$ and denote the corresponding web spaces by $\Gamma_{q=1}^{\mathcal{W}_{2n}}$ and $\Gamma_{q=1}^{\mathcal{W}_{3n}}$.

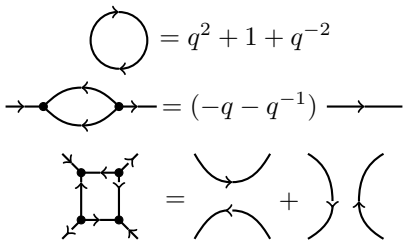

FIGURE 2. Relations on $\mathfrak{sl}_3$ webs

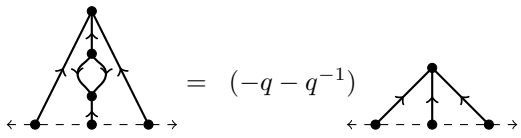

FIGURE 3. Reducing an $\mathfrak{sl}_3$ web

Definition 2.3. Given a face of a bottom web, we define its *depth* to be the minimum number of edges a path to the unbounded face must cross. (Paths are not permitted to pass through vertices of the web.) This is well-defined as it is a distance between vertices in the web's dual graph.

Using face depths depth, one can associate a symbol to each boundary vertex where + indicates that the depth immediately to the left of the vertex is smaller than the depth to the right, 0 indicates that these two depths are equal, and − indicated that the depth to the left is larger than the depth to the right. The resulting string of symbols read left to right is called the boundary word for the web. Figure 4 has an example of a web and its boundary word.

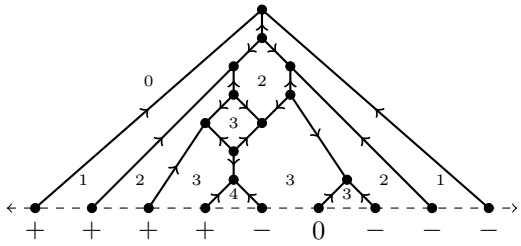

FIGURE 4. An unreduced $\mathfrak{sl}_3$ web and its boundary word.

Definition 2.4. Let S be a string of symbols in the alphabet $\{s_1, \ldots, s_n\}$. Given $1 \leq i, j \leq n$, we say S is $(s_i s_j)$-*balanced* if it has the same number of s_i and s_j symbols and $(s_i s_j)$-*Yamanouchi* if, reading left to right, the number of s_j symbols at any point does not exceed the number of s_i symbols. Note that the order of symbols matters in the definition of Yamanouchi but not balanced. (i.e. $(s_i s_j)$-balanced is the same thing as $(s_j s_i)$balanced, but $(s_i s_j)$-Yamanouchi is not the same as $(s_j s_i)$-Yamanouchi.)

Boundary words for webs are key to connecting them to tableaux. The following two results have been shown in previous papers about web combinatorics and also follow from the discussion on band diagrams for half plane graphs in Section 3 below.

Theorem 2.5. *The boundary words for webs in $\mathcal{W}_{2n}$ are in the alphabet $\{+, -\}$ and are both $(+-)$-balanced and $(+-)$-Yamanouchi.*

Theorem 2.6. *The boundary words for webs in $\mathcal{W}_{3n}$ are in the alphabet $\{+, 0, -\}$ and are both $(+-)$-balanced and $(+-)$-Yamanouchi. Reduced webs in $\mathcal{W}_{3n}$ have boundary words that are also $(+0)$ and $(0-)$-balanced as well as $(+0)$ and $(0-)$-Yamanouchi.*

2.2. **Tableaux and Webs.**

Definition 2.7. Given $m \in \mathbb{N}$ and a partition $\lambda = (\lambda_1, \ldots, \lambda_t) \vdash m$, we define

- the *Young diagram of shape* λ to be the top and left justified collection of m boxes where the i^{th} row has λ_i boxes,
- a *Young tableau of shape* λ to be a filling of the boxes of the Young diagram of shape λ with the numbers 1 through m each occurring exactly once, and
- a *standard Young tableau of shape* λ to be a Young tableau of shape λ in which the numbers increase from left to right along rows and top to bottom along columns.

We denote the set of all standard Young tableaux of shape λ by $SYT(\lambda)$.

Let $\mathcal{W}_{2n}^R$ be the set of reduced webs in $\mathcal{W}_{2n}$, and define the map $\psi : \mathcal{W}_{2n}^R \to SYT(n,n)$ such that $\psi(w)$ is the tableau obtained by writing i in the top (resp. bottom) row if the i^{th} symbol in the boundary word for w is $+$ (resp. $-$). It is a straightforward exercise to show that $\psi(w)$ is indeed standard and that ψ is a bijection.

To explicitly describe the web $\psi^{-1}(T)$ giveb $T \in SYT(n,n)$, first construct a word in the alphabet $\{+,-\}$ from T such that the i^{th} symbol is $+$ if i is in the top row of T and $-$ if i is in the bottom row. This word will be $+-$-balanced and $+-$- Yamanouchi by construction. There is a unique reduced $\mathfrak{sl}_2$ web on $2n+0$ boundary points with that band word. Figure 5 has an example summarizing these relationships.

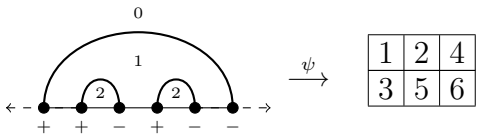

FIGURE 5. An $\mathfrak{sl}_2$ web, boundary word, and tableau

In an analogous setup, let $\mathcal{W}_{3n}^R$ be the set of reduced webs in $\mathcal{W}_{3n}$, and define the map $\psi : \mathcal{W}_{3n}^R \to SYT(n,n,n)$ such that $\psi(w)$ is the tableau obtained by writing i in the top (resp. middle, resp. bottom) row if the i^{th} symbol in the boundary word for w is $+$ (resp. 0, resp. $-$). This bijection is due to Khovanov-Kuperberg [**?**, paper]

Explicitly constructing $\psi^{-1}(T)$ for $T \in SYT(n,n,n)$ involves an intermediate object called an M-diagram [**?**]. As in the $\mathfrak{sl}_2$ case, begin by constructing a word in $\{+,-,0\}$ with $+$ corresponding to top row, 0 corresponding to middle, and $-$ to bottom of T. Since T is standard, the resulting word is $(+,0)$, $(+,-)$ and $(0,-)$- balanced as well as $(+,0)$, $(+,-)$ and $(0,-)$-Yamanouchi.

Next, label the vertices $1, \ldots 3n$ on a horizontal axis with the corresponding symbols in word coming from T. The M-diagram for T is a pair of crossingless matchings on these labeled points. One matching on the vertices labeled $+$ and 0 has left endpoints labeled $+$ and right endpoints labeled 0. The other matching has left endpoints labeled 0 and right endpoints labeled $-$. There are unique matchings with these properties, so the M-diagram is unique. Note that while each matching is crossingless, the arcs from one matching can intersect the other. As we will see later, M-diagrams are not only useful in this algorithm but are also used to track combinatorial statistics for webs.

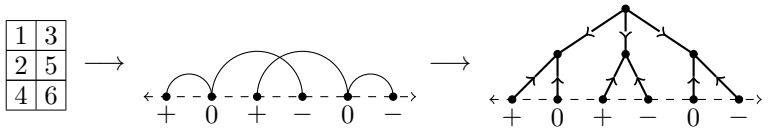

FIGURE 6. Constructing an $\mathfrak{sl}_3$ web from a tableau

Finally, to obtain a web from an M-diagram, orient all arcs of the M-diagram away from boundary vertices labeled $+$ and $-$, and modify crossings and neighborhoods of boundary vertices labeled 0 as shown in Figure 7. Note that this figure also labels local depths around these areas of modification. These will be used later. Figure 6 has an example of a 3-row tableau and its companion diagrams.

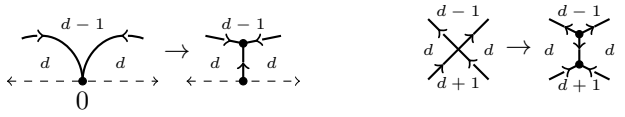

FIGURE 7. Constructing a web from an oriented M-diagram

3. Half-plane graphs

Half-plane graphs are generalizations of webs. In this section, we define half-plane graphs, construct their band diagrams, study combinatorial properties of band diagrams, and connect them to the web combinatorics described above.

3.1. **Band diagrams for half-plane graphs.**

Definition 3.1. A *half-plane graph G^+ with n boundary vertices* is a plane graph (i.e. planar graph with choice of embedding) with vertex set $V = \{1, 2, \ldots, n\} \cup V_{int}$ and edge set E with the properties that

(1) E contains exactly one edge incident to each vertex $\{1, 2, \ldots, n\}$,
(2) All edges have distinct endpoints,
(3) Vertices in V_{int} are trivalent, and
(4) The graph can be drawn so that
   - the vertices $\{1, 2, \ldots, n\}$ are the associated integers on the x-axis of the plane, and
   - the vertices V_{int} are all in the the upper half of the plane.

The *faces of G^+* are the path-connected, open subsets of the complement of G^+ in the upper half-plane.

In the context of this paper, $\mathfrak{sl}_2$ and $\mathfrak{sl}_3$ bottom webs are the most relevant examples of half-plane graphs. One obtains an $\mathfrak{sl}_2$ web whenever $V_{int} = \emptyset$. When n is divisible by 3 and the edges can be oriented so that each internal vertex is either a source or sink, one obtains an $\mathfrak{sl}_3$ web. Figure 8 has an example of a half-plane graph that is not a web.

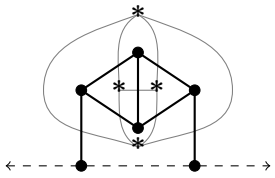

FIGURE 8. A half-plane graph and its dual.

Definition 3.2. Let G^+ be a half-plane graph. Given a face F of G^+, the *depth of F* is the distance (i.e. minimal path length) in the dual graph $(G^+)^*$ from the vertex F^* to the vertex corresponding to the unbounded face of G^+. Depth is well-defined and finite because $(G^+)^*$ is well-defined and connected.

Definition 3.3. Associated to a half-plane graph G^+, we define the following subsets of the upper half-plane.

- Given a nonnegative integer d, the *d-band of G^+* is the closure of the union of all faces of depth d. (We refer to the connected components of the d-band simply as the *components of the d-band.*)
- Given a nonnegative integer d, the *d-arc of G^+* is the intersection of the d-band and the $(d-1)$-band. (We refer to the connected components of the d-arc simply as the *components of the d-arc.*)
- The *band diagram for G^+*, denoted $B(G^+)$ is the union of the d-arcs of G^+ over all nonnegative integers d.
- The *anchored band diagram for G^+*, denoted $B_A(G^+)$, is the band diagram for G^+ minus any closed components. (If a band diagram has no closed components, in other words $B(G^+) = B_A(G^+)$, we say the band diagram is *anchored.*)

As an example, the 0-band of the half-plane graph shown in Figure 8 is the closure of the unbounded face, and the 1-band is closure of the union of all bounded faces. The 1-arc, band diagram, and anchored band diagram are all equal in this case and consist of the edges of the graph adjacent to both the unbounded face and some bounded face.

Say i is a boundary vertex for a half-plane graph G^+. There is a unique edge incident to i separating two faces. These faces necessarily have depths $d-1$ resp. d, d resp. d, or d resp. $d-1$ for some nonnegative integer d. We use the relationship between these faces to construct a boundary word for a half-plane graph.

Definition 3.4. Given a half-plane graph G^+, label its boundary vertices $+$, 0, or $-$ based on whether depth of the face immediately to the left of the vertex is smaller, the same, or larger than the depth to the right. We call the resulting string of symbols read left to right the *boundary word* for a half-plane graph.

Lemma 3.5. *The boundary word for a half-plane graph is $(+-)$-balanced and $(+-)$-Yamanouchi.*

Proof. Given a half-plane graph with n boundary vertices, there are $n+1$ faces touching the x-axis. Considering these face depths as we traverse the axis from left to right, depth begins and ends at zero, is never negative, and increases or decreases by one or zero at each boundary point. Hence the boundary word must be $(+-)$-balanced. Since depth is nonnegative, the number of $+$ symbols at any point in the boundary word must always be greater than or equal to the number of $-$ symbols. We conclude the boundary word is $(+-)$-Yamanouchi. □

Proposition 3.6. *The d-arc of a half-plane graph is a 1-manifold with boundary on the x-axis.*

Proof. The d and $d-1$ bands intersect along edges of G^+, so the d-arc is necessarily the union of a subset of edges of G^+. We will show if one edge incident to an internal vertex is part of the d-arc then exactly two edges at that vertex are part of the d-arc. It follows from this fact that each d-arc component is either a closed one-manifold passing through a subset of the internal vertices of G^+ or a path between boundary vertices possibly passing through intermediate internal vertices.

The depths of faces that share an edge in G^+ can differ by at most one. Therefore either

(i) the depths of the three faces around an internal vertex are all the same or

(ii) two of the three faces around an internal vertex are the same and the third depth differs by one. This is shown in Figure 9.

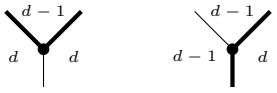

FIGURE 9. The d-arc near an internal vertex

No edges incident to vertices of type (i) can be part of the d-arc. If an edge incident to a vertex of type (ii) is part of the d-arc, Figure 9 shows exactly two edges incident to that vertex are part of the d-arc. □

Remark 3.7. Trivalency is essential in Proposition 3.6. To illustrate this, consider the following example which satisfies all properties of being a half-plane graph except trivalency of internal vertices. Since all edges separate faces of different depths, every edge of this graph would be part of the band diagram.

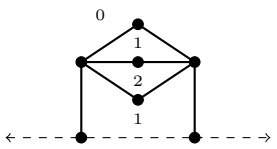

FIGURE 10. Nonexample of a half-plane graph

Proposition 3.8. *The anchored band diagram of a half-plane graph is a crossingless matching on the boundary vertices labeled $+$ and $-$.*

Proof. By construction, the anchored band diagram is the union of nonintersecting, connected 1-manifolds each of which is homeomorphic to an interval and has both endpoints on the axis of the half-plane graph. This is exactly a crossingless matching. □

Proposition 3.9. *The left (resp. right) endpoints of the band diagram for a half-plane graph are labeled + (resp. −).*

Proof. Consider a curve c in the anchored band diagram for a half-plane graph; then c is a component of the d-arc for some d. The curve c connects two points on the x-axis and splits the upper half-plane into two regions – one above and one below c. The region above c includes the unbounded face. The d-arc is the intersection of the d-band and $(d-1)$-band, so the faces adjacent to c on one side have depth $d-1$ and on the other side have depth d.

Every path to the unbounded face from a face adjacent to and below c must cross c and enter a face adjacent to and above c. It follows that the faces of depth d are below c. This means the left endpoint of c is labeled + indicating an increase in depth while the right endpoint is labeled − indicating a decrease in depth. □

Given a $(+-)$-balanced, $(+-)$-Yamanouchi word in the alphabet $\{+,-\}$, we observed earlier that there is a unique crossingless matching pairing these points such that left endpoints are labeled + and right endpoints are labeled −. This leads to the following corollary of Proposition 3.9.

Corollary 3.10. *The anchored band diagram of a half-plane graph is determined up to isotopy by its boundary word.*

Definition 3.11. Given a half-plane graph G^+, the *shadow* of G^+ is a nested collection of sets

$$S(G^+) : S_1(G^+) \supseteq S_2(G^+) \supseteq S_3(G^+) \supseteq \cdots$$

where $S_d(G^+)$ is the set of all points on the real axis of the upper half-plane belonging to a k-band for some $k \geq d$.

Remark 3.12. We make the following useful observations about the shadow of a half-plane graph G^+.

- If a band diagram is drawn using half circles, then $S_d(G^+)$ is the result of orthogonally projecting the d-arcs in the band diagram to the real axis.
- For all d, S_d is the union of finitely many closed intervals.

Figure 11 shows a half-plane graph on 6 boundary vertices with face depths labeled and its band diagram highlighted in red. The shadow for this graph is $S : [1,6] \supset [3,4]$.

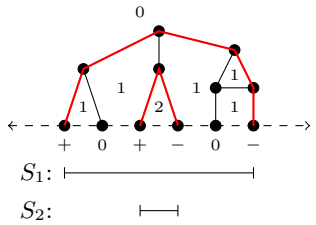

FIGURE 11. A half-plane graph and its shadow

We conclude this subsection with one final definition that will lead to a partial order on half-plane graphs.

Definition 3.13. Given two half-plane graphs G_1^+ and G_2^+, we will say $S(G_1^+) \subset S(G_2^+)$ if $S_d(G_1^+) \subset S_d(G_2^+)$ for all d.

The next lemma follows immediately from the definitions of shadows and shadow containment.

Lemma 3.14. *Given two half plane graphs G_1^+ and G_2^+ with the same number of boundary vertices, $S(G_1^+) \subset S(G_2^+)$ if and only if the depth at every point along the x-axis in G_1^+ is at most the depth at the same point on the x-axis in G_2^+.*

3.2. **Band diagrams for webs.** Every bottom web is a half-plane graph. We can therefore associate a band diagram to each bottom web. We will see that for reduced $\mathfrak{sl}_2$ webs, the band diagram is trivial. For $\mathfrak{sl}_3$ webs, however, the band diagram has some interesting properties.

Recall that an $\mathfrak{sl}_2$ bottom web is a half-plane graph with no internal vertices. Further, each arc in an $\mathfrak{sl}_2$ web separates faces of different depth, so the band diagram for an $\mathfrak{sl}_2$ bottom web is the web itself. Trivially, then, an $\mathfrak{sl}_2$ bottom web is completely determined by its band diagram. The band diagram for an $\mathfrak{sl}_2$ web is anchored if and only if it is reduced.

Unlike $\mathfrak{sl}_2$ webs, $\mathfrak{sl}_3$ webs can have edges between faces of the same depth, so their band diagrams are more complicated to characterize. Figure 12 has an example of a reduced $\mathfrak{sl}_3$ web and its band diagram. We will show in the next proposition that a reduced $\mathfrak{sl}_3$ web has an anchored band diagram.

Proposition 3.15. *The band diagram for any reduced $\mathfrak{sl}_3$ bottom web is anchored.*

Proof. Tymoczko shows that the depth of a face of a reduced web is equal to the number of arcs above the corresponding face in the M-diagram. The local depths around internal vertices of reduced webs are as shown in Figure 7. From this figure, we see that vertical edges are never part of a band diagram for a web constructed in this way. It is thus impossible for the band diagram for a reduced $\mathfrak{sl}_3$ web to have closed components. □

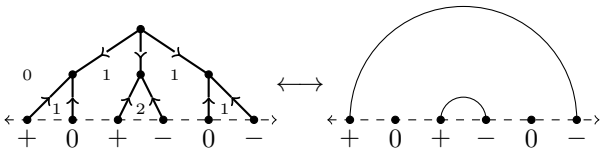

FIGURE 12. A band diagram for an $\mathfrak{sl}_3$ web

An immediate consequence of Proposition 3.15 and Corollary 3.10 is that the band diagram for a reduced $\mathfrak{sl}_3$ bottom web can be constructed directly from its tableau. This means that a reduced $\mathfrak{sl}_3$ bottom web is uniquely determined by its band diagram and therefore uniquely determined by its shadow.

We make one final observation about $\mathfrak{sl}_3$ web shadows that will be useful in upcoming sections. Given an arbitrary $\mathfrak{sl}_3$ bottom web, it can be expressed uniquely as a linear combination of reduced webs. One accomplishes this via a sequence of reductions using the rules in Figure 2. Since these relations remove edges, the depths at every point along the boundary in webs coming from reduction are always less than or equal to those of the original web. Hence, we obtain the following useful result.

Lemma 3.16. *Let w be an unreduced $\mathfrak{sl}_3$ bottom web with $w = \sum_{i=1}^{t} c_{\widetilde{w}_i} \widetilde{w}_i$ where $\widetilde{w}_i$ is reduced for all i. Then $S(\widetilde{w}_i) \subseteq S(w)$ for all i.*

Remark 3.17. Unreduced $\mathfrak{sl}_3$ webs have messier combinatorics. The boundary word for such a web is guaranteed to be $(+,-)$-balanced and $(+-)$-Yamanouchi but will not necessarily be $(+0)$ or $(0-)$-balanced nor $(+0)$ or $(0-)$-Yamanouchi. Figure 4 has an example.

The band diagram for an unreduced $\mathfrak{sl}_3$ web is not necessarily anchored. Figure 3 shows an example of an unreduced web whose band diagram is not anchored and the unique reduced web that shares its band word.

Band diagrams and boundary words uniquely identify reduced $\mathfrak{sl}_3$ bottom webs but not $\mathfrak{sl}_3$ bottom webs in general. There exist webs with the same boundary word and even webs with the same band diagram. The webs in Figure 3 have the same boundary word but not the same band diagram. The webs in Figure 13 have the same band diagram and hence the same boundary word.

Remark 3.18. Reduced $\mathfrak{sl}_3$ bottom webs with arbitrary boundary orientation are in bijection with certain semistandard Young tableaux of rectangular shape. These webs can be viewed as contractions of the reduced $\mathfrak{sl}_3$ webs with $3n$ boundary vertices that are all sources. Since these reduced webs can be obtained via contraction, they also have anchored band diagrams.

FIGURE 13. Two $\mathfrak{sl}_3$ bottom webs with the same band diagram.

4. A partial order on webs coming from tableaux

In this section, we construct a partial orders on webs coming from tableaux. In the next section, we introduce another partial order on webs coming from band diagrams and compare them. In the last section, we will apply these partial orders to describe the coefficients in the transition matrix between two bases for the same symmetric group representation: the Specht basis which is indexed by SYT and the web basis.

Let $m \in \mathbb{N}$ and let $s_i \in S_m$ be the simple transposition in the symmetric group on m letters that interchanges i and $i+1$. The symmetric group acts on tableaux by permuting entries. Given a tableau T of shape $\lambda \vdash m$, define $s_i \cdot T$ to be the tableau obtained by swapping entries i and $i+1$ in T and leaving all other entries fixed. Note that this action does not in general preserve standardness.

Using this symmetric group action, define a partial order on the set of SYT of any fixed shape λ as follows.

Definition 4.1. Given standard Young tableaux T and T' of shape λ, we say

- $T \to T'$ if there exists i such that $T' = s_i \cdot T$ and i is in a row above $i+1$ in T' (We sometimes write $T \xrightarrow{s_i} T'$ in this case), and
- $T \prec T'$ if there exist $T_1, \ldots, T_k$ such that $T \to T_1 \to \cdots \to T_k \to T'$.

The arrows $T \to T'$ form the edges of the Hasse diagram for this partial order. An example is shown in Figure 14. (Note that we draw the Hasse diagram with descending edges.) In the case of rectangular partitions, the Hasse diagram for this partial order is connected with unique maximal and minimal elements. The minimal element is the column-filled tableau and the maximal one is the row-filled tableau.[**?**]

This poset on tableaux is ranked [**?**]. By construction, the rank function is given by the number of descents in a tableau.

Definition 4.2. Given a tableau $T \in SYT(\lambda)$,

- the *column word* for T is the sequence of integers obtained by reading down the columns of T from left to right beginning with the leftmost column, and
- a *descent* in the column word for T is an instance where $i < j$ but j appears before i in the column word.

For instance, in Figure 14, the column word for the top tableau is 123456 which has no descents, and the column word for the bottom tableau is 142536 which has 3 descents.

Given $n \in \mathbb{N}$, we can use the bijections $\psi^{-1} : SYT(n,n) \to \mathcal{W}_{2n}^R$ and $\psi^{-1} : SYT(n,n,n) \to \mathcal{W}_{2n}^R$ and the partial order on tableaux to endow webs with a partial order we denote by $\prec_T$. In other words, given reduced webs w, w' with the same boundary such that $\psi(w) = T$ and $\psi(w') = T'$, we say $w \prec_T w'$ if and only if $T \prec T'$.

In the $\mathfrak{sl}_2$ case, the Hasse diagram for $\prec_T$ has a straightforward description on the level of webs. Given reduced webs $w, w' \in \mathcal{W}_{2n}^R$, there exists an edge $w \to w'$ if and only if there are i, j, and k such that w and w' are identical on all vertices except $j < i < i+1 < k$ and w pairs (j,i) and $(i+1,k)$ whereas w' pairs (j,k) and $(i,i+1)$. Figure 14 gives a summarizing example.

In the $\mathfrak{sl}_3$ case, we have discussed three different combinatorial objects associated to $T \in SYT(n,n,n)$: a web, an M-diagram, and a band diagram. Via the bijection ψ^{-1} and the partial order on tableaux, we therefore obtain partial orders not just on webs but also on M-diagrams and band diagrams. In all cases, we denote this partial order by $\prec_T$. This is shown in Figure 15 in the $(2,2,2)$ case.

Since the tableaux poset is ranked, $\prec_T$ is also a ranked partial order. There are several rank functions for $\prec_T$ each of which we denote by r. The formulas for r depend on various statistics on webs, M-diagrams, and band diagrams which we will now define.

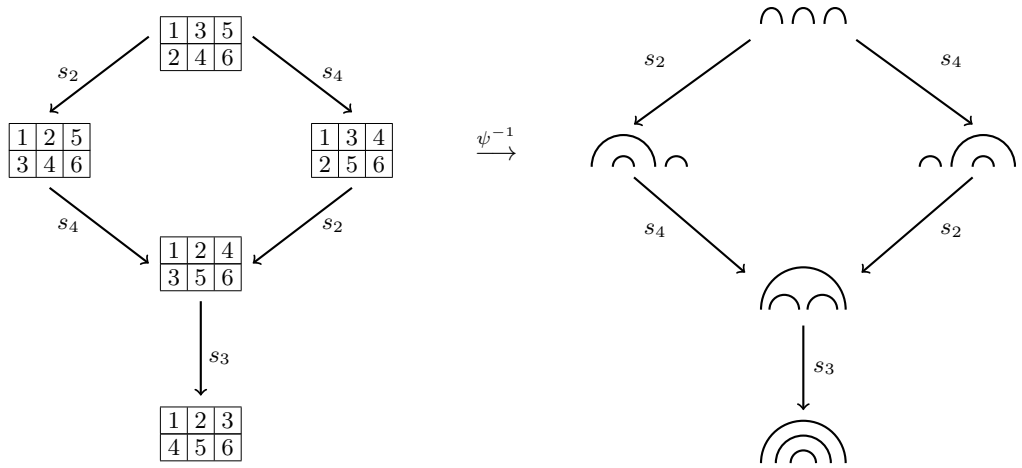

FIGURE 14. The poset structure on webs and tableaux corresponding to shape $(3,3) \vdash 6$

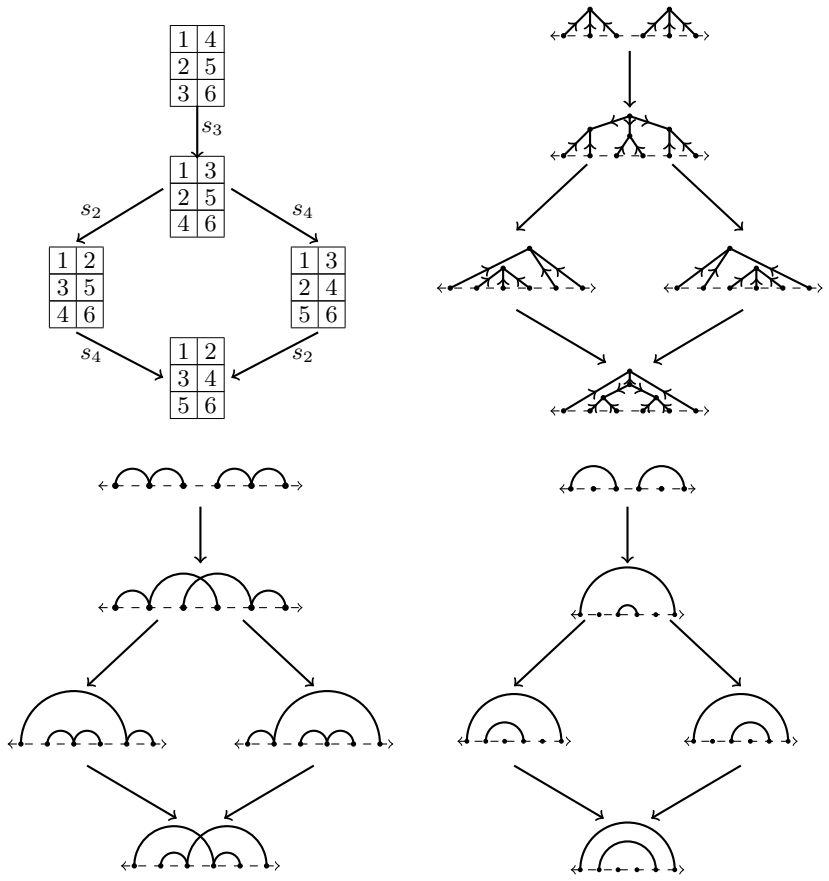

FIGURE 15. The poset structure on webs, tableaux, M-diagrams, and band diagrams in the $(2,2,2) \vdash 8$ case

Definition 4.3. Let D be an $\mathfrak{sl}_2$ web, an M-diagram for an $\mathfrak{sl}_3$ web, or a band diagram. In each case, D has an associated set of arcs. For an arc a in D, we write $a \in D$.

- For each $a \in D$, the *nesting number of* a, written $n(a)$, is the number of arcs in D above a that do not intersect a.
- The *nesting number for* D, written $n(D)$, is the sum of its nesting numbers. i.e. $n(D) = \sum_{a \in D} n(a)$.

Definition 4.4. Let B be a band diagram for a half-plane graph with m boundary vertices.

- For $1 \leq i \leq m$, we define the *dot depth of* i *in* B, written $d(i)$, to be 0 if i is the boundary of an arc in B and the number of arcs of B above i otherwise.
- The *dot depth of* B, written $d(B)$, is the sum $d(B) = \sum_{i=1}^{m} d(i)$.

We use the language of dots since they correspond to unpaired vertices on the x-axis.

Definition 4.5. Given an M-diagram M for an $\mathfrak{sl}_3$ web, we define the *crossing number of* M to be the number of intersections of arcs in the interior of the diagram. (We do not count the boundary points labeled 0 as crossings.)

Definition 4.6. Let w be an $\mathfrak{sl}_3$ bottom web. For a face F of w, we will write $F \in w$.

- We denote the depth of F in w by $d(F)$.
- The face F is called *excluded* if it is the unique lowest depth face around some internal vertex of w. (Note that not all internal vertices of w are adjacent to an excluded face.) Denote by $E(w)$ the set of excluded faces.

Using these quantities, we can prove the following lemma which provides several formulas to compute the rank function r for $\prec_T$. The formulas using M-diagrams and band diagrams can be proven via straightforward inductive arguments. The formula on webs comes from the observation that crossings in M-diagrams correspond to trivalent source vertices in the associated web, and arcs in the M-diagram are in bijection with bounded faces of w that are not excluded.

Lemma 4.7. *Given $w \in \mathcal{W}_{2n}^R$, $r(w) = n(w)$. In other words, the rank of w is its nesting number.*

Lemma 4.8. *Let $w \in \mathcal{W}_{3n}^R$, and let B and M be the band and M-diagrams associated to w. By definition $r(w) = r(B) = r(M)$. Further, the following are all rank functions for $\prec_T$.*

- *On the level of M-diagrams, $r(M) = n(M) + c(M)$. In other words, rank is the sum of the nesting number and crossing number of an M-diagram.*
- *On the level of band diagrams, $r(B) = n(B) + d(B) - n$. In other words, rank is the sum of the nesting number and dot depth of a band diagram minus n.*
- *Say w has $s(w)$ internal source vertices. Then we have the following rank function on the level of webs.*

$$r(w) = s(w) + \sum_{\substack{F \in w \\ F \notin E(w)}} d(F)$$

In other words, rank is the sum of the depths of the non-excluded faces plus the number of internal source vertices.

Remark 4.9. The rank functions on band diagrams and webs can be extended to unreduced webs. We have not checked if they are equal in this more general setting. The rank function on band diagrams can be even further generalized to any half-plane graph though it is not clear which integer should be subtracted in this case.

5. A partial order on webs coming from band diagrams

Recall given two half-plane graphs G_1^+ and G_2^+, we say $S(G_1^+) \subset S(G_2^+)$ if $S_d(G_1^+) \subset S_d(G_2^+)$ for all d. This notion of shadow containment leads to a partial order on webs.

Definition 5.1. Let $w, w' \in \mathcal{W}_{2n}^R$ or $w, w' \in \mathcal{W}_{3n}^R$ be a pair of reduced bottom webs of the same type. We say $w \prec_S w'$ if $S(w) \subset S(w')$. We will sometimes refer to this as the *shadow containment* partial order.

Remark 5.2. We cannot extend the partial order $\prec_S$ to all half-plane graphs or even to unreduced webs since these larger collections have distinct half-plane graphs with the same shadow. See Remark 3.17 above for more detail on this phenomenon for unreduced webs.

The following lemma is an immediate consequence of the definition of the shadow of a half-plane graph and will be useful in our analysis of shadow containment.

Lemma 5.3. *Given two webs w and w', $w \prec_S w'$ if and only if the depth at every point on the boundary of w is no greater than the depth at the corresponding point in w'.*

We are interested in comparing $\prec_T$ to $\prec_S$ on the sets $\mathcal{W}_{2n}^R$ and $\mathcal{W}_{3n}^R$. We will show that these partial orders coincide for reduced $\mathfrak{sl}_2$ webs but differ for $\mathfrak{sl}_3$ webs. In fact, the shadow containment partial order on $\mathfrak{sl}_3$ webs fails to be ranked.

5.1. **Shadows of $\mathfrak{sl}_2$ webs.** All webs in this subsection are reduced $\mathfrak{sl}_2$ bottom webs. This means they are crossingless matchings with no additional closed components. We are interested in exploring $\prec_S$ for these webs. As an example, let w' consist of arcs $(1,4)$ and $(2,3)$ and w consist of arcs $(1,2)$ and $(3,4)$. Then $S_1(w') = [1,4]$, $S_2(w') = [2,3]$, and $S_d(w') = \emptyset$ for all $d > 2$. For w, we have $S_1(w) = [1,2] \cup [3,4]$ and $S_d(w) = \emptyset$ for all $d > 1$. It follows that $S(w) \subset S(w')$ so $w \prec_S w'$.

The next lemma describes what we see in this example and follows immediately from the definition of nesting number and the fact that the band diagram for a reduced $\mathfrak{sl}_2$ bottom web is the web itself.

Lemma 5.4. *Let $(i_1, j_1), \ldots, (i_t, j_t)$ be the list of all arcs with nesting number d in a web w. Then $S_{d+1}(w) = [i_1, j_1] \cup \cdots \cup [i_t, j_t]$. In other words, the intervals in $S(w)$ are in bijection with the arcs of w, and they are partitioned according to nesting number.*

Given $w \in \mathcal{W}_{2n}^R$, recall $r(w)$ is the sum of the nesting numbers of the arcs of w. We will prove a sequence of lemmas relating $\prec_T$ and $\prec_S$ for reduced $\mathfrak{sl}_2$ bottom webs.

Lemma 5.5. *Let $w, w' \in \mathcal{W}_{2n}^R$. If $w \prec_S w'$, then $r(w) < r(w')$.*

Proof. Let $w, w' \in \mathcal{W}_{2n}^R$ with $S(w) \subset S(w')$. Rather than a sum over arcs of a web, we may think of the rank function r as a sum over endpoints of a web where we count $\frac{d}{2}$ for each endpoint of an arc of nesting number d. Every arc in an $\mathfrak{sl}_2$ web separates two neighboring faces with depths that differ by one, and the smaller of those depths is the nesting number of the arc. Integral points in the interval $[1, 2n]$ are in bijection with the arc endpoints in the boundaries of w and w', so another way to think of $r(w)$ and $r(w')$ is as a sum over each integral boundary point of the web of $\frac{d}{2}$ where d is the minimum depth in a small neighborhood of that point.

By Lemma 5.3, since $S(w) \subset S(w')$, the depth at any point on the boundary of w is no larger than the depth at the same point in w'. It follows that $r(w') \geq r(w)$. Since containment is proper, there is at least one integral boundary point, say i, around which the shadows of w and w' differ. WLOG, say the depth in w' at $i - \frac{1}{2}$ is $d-1$ and at $i + \frac{1}{2}$ is d. Then i contributes $\frac{d-1}{2}$ to $r(w')$. Say the depth in w at $i - \frac{1}{2}$ is d' and at $i + \frac{1}{2}$ is d''. This is shown in Figure 16.

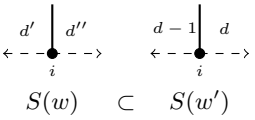

FIGURE 16. Local depths in the $S(w) \subset S(w')$ case

The shadows differ, so either $d - 1 \neq d'$ or $d \neq d''$ (or both). Since $S(w) \subseteq S(w')$, we know $d - 1 \geq d'$ and $d \geq d''$. Since i is an arc endpoint in w, we know $|d' - d''| = 1$. Combining these conditions, if $d - 1 = d'$, then $d'' = d - 2$. Otherwise, $d - 1 > d'$. In either case, the integral point i contributes less than $\frac{d-1}{2}$ to $r(w)$, and we see $r(w') > r(w)$. □

Lemma 5.6. *If $w \prec_T w'$, then $w \prec_S w'$.*

Proof. If $w \prec_T w'$, then there is a directed path in the Hasse diagram for $\prec_T$ from w to w'. We will show that for an edge $w \to w'$ in the Hasse diagram for $\prec_T$, it is always true that $w \prec_S w'$. Once this is established, the lemma follows by induction on path length.

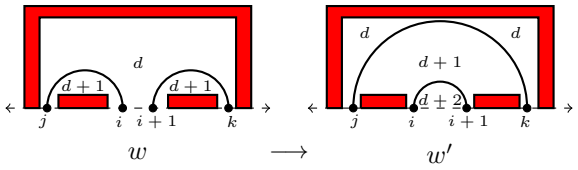

FIGURE 17. Depth change along an edge in the Hasse diagram

If $w \to w'$, then w and w' are identical except for two arcs on four integral boundary points $j < i < i+1 < k$ where w has arcs (j, i) and $(i+1, k)$ and w' has arcs (j, k) and $(i, i+1)$. Figure 17 illustrates this relationship using red regions to represent the locations of arcs common to w and w'.

It is easy to check the depths along the boundaries of w' and w are the same except between boundary points i and $i+1$. If the depth between i and $i+1$ in w is d, then it is $d+2$ in w'. It follows that $S_i(w) = S_i(w')$ for $i \neq d+1, d+2$ and $S_i(w) \cup [i, i+1] = S_i(w')$ for $i = d+1, d+2$. Hence $w \prec_S w'$. □

Lemma 5.7. *If $w \prec_S w'$, then $w \prec_T w'$.*

Proof. We will argue via double induction. One can explicitly check this result is true for all pairs of webs in $\mathcal{W}_{2n}^R$ where $n = 1, 2, 3$. Now assume that for all pairs of webs with fewer than n arcs, if $w \prec_S w'$, then $w \prec_T w'$.

Let w and w' be webs with n arcs such that $w \prec_S w'$. Consider the arc $(1, j)$ in w' which necessarily has nesting number 0, and say w has $k+1$ arcs of nesting number 0 with both endpoints in the interval $[1, j]$. If $k = 0$, then w and w' both have the arc $(1, j)$. In this case, we can remove this arc from both matchings and maintain shadow containment. What remains is a pair of webs with $n-1$ arcs, and the inductive hypothesis implies $w \prec_T w'$.

Now say w has arcs $(1, t_1), (t_1 + 1, t_2), (t_2 + 1, t_3), \ldots (t_k + 1, t_{k+2}) = (t_k + 1, j)$ where $k \geq 1$. Note that each of these arcs necessarily has nesting number 0 in w. The endpoint $t_{k+2} = j$ must be even since the points below the arc $(1, j)$ are paired in w'. In fact, arc endpoints will always have opposite parity for this reason, and, moreover, left endpoints of even nesting number arcs must be odd while left endpoints of odd nesting number arcs must be even. This implies that, for each even endpoint $2m$ strictly between 1 and j, $[2m, 2m+1] \subset S_2(w')$, otherwise, $2m+1$ would be a left endpoint of a nesting number 1 arc. Since $S_2(w') \subset S_1(w')$, it also follows that $[2m, 2m+1] \subset S_1(w')$.

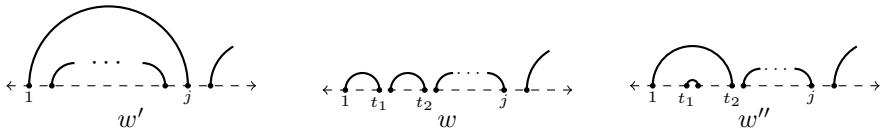

FIGURE 18. Webs w, w', and w''

Let w'' be the web with arcs $(1, t_2)$ and $(t_1, t_1 + 1)$ that otherwise does not differ from w. Local pictures of w, w', and w'' are shown in Figure 18. Then there is an edge $w \to w''$ in the Hasse diagram for $\prec_T$. We know from the proof of Lemma 5.6 that $w \prec_S w''$. In fact, we know exactly how the shadows of w and w'' differ. In particular, they are exactly the same except $[t_1, t_1 + 1]$ has depth 2 in w'', and therefore $S_i(w'') = S_i(w) \cup [t_1, t_1 + 1]$ for $i = 1, 2$ and $S_i(w'') = S_i(w)$ for all $i > 2$.

Since t_1 was a right endpoint of an arc of nesting number 0 in w, we know t_1 is even. Therefore $[t_1, t_1+1] \subset S_i(w')$ for $i = 1, 2$. It follows that $S(w'') \subset S(w')$, so $w'' \prec_S w'$. Further, note that with w'' has one fewer arc of nesting number 0 with endpoints between 1 and j. By induction on k, we have $w'' \prec_T w'$. Since $w \prec_T w''$ and $w'' \prec_T w'$, we conclude $w \prec_T w'$. □

Theorem 5.8. *Let $w, w' \in \mathcal{W}_{2n}^R$. Then $w \prec_S w'$ if and only if $w \prec_T w'$. In other words, the partial orders $\prec_T$ and $\prec_S$ coincide on the set $\mathcal{W}_{2n}^R$.*

5.2. $\mathfrak{sl}_3$ **web shadows.** In this subsection, we show the shadow containment partial order is not the same as the tableaux partial order for reduced $\mathfrak{sl}_3$ webs. In fact, the partial order $\prec_S$ is not even ranked in the $\mathfrak{sl}_3$ web case.

We accomplish this in two steps. First, we prove the covering relation for $\prec_S$ contains the covering relation for $\prec_T$. This implies that if $\prec_S$ were ranked, then it would have the same rank function as $\prec_T$. We conclude with an example of reduced $\mathfrak{sl}_3$ webs w and w' with $w \prec_S w'$ and $r(w) > r(w')$.

Lemma 5.9. *Let $w, w' \in \mathcal{W}_{3n}^R$ such that $w \to w'$ be an edge in the Hasse diagram for $\prec_T$. Then $w \prec_S w'$, and there does not exist web $\overline{w}$ such that $w \prec_S \overline{w} \prec_S w'$. Hence the covering relation for $\prec_T$ is a subset of the covering relation for $\prec_S$.*

Proof. Let $w, w' \in \mathcal{W}_{3n}^R$ such that $w \to w'$ is an edge in the Hasse diagram for $\prec_T$. It follows that webs w and w' have identical Yamanouchi words in all but two adjacent positions i and $i+1$ for some $1 < i < 3n$. The depths along the boundaries of w and w' are therefore identical except between the boundary vertices i and $i+1$.

According to the definition of the partial order $\prec_T$, the Yamanouchi symbols for w and w' in positions i and $i+1$ must be related according to one of the cases listed in the table in Figure 19. In the first two cases, the depth between i and $i+1$ in w' is one greater than in w. In the final case, the depth between i and $i+1$ in w' is two greater than in w.

	Y-word for w	**Y-word for w'**
Case 1:	$0+$	$+0$
Case 2:	-0	$0-$
Case 3:	$-+$	$+-$

FIGURE 19. i^{th} and $(i+1)^{st}$ Yamanouchi symbols along edge $w \xrightarrow{s_i} w'$

Given a reduced $\mathfrak{sl}_3$ web $\widetilde{w}$ such that $w \preceq_S \overline{w} \preceq_S w'$, the depth at each point along the boundary of $\overline{w}$ is bounded below by the corresponding depth in w and above by the depth in w'. It follows that the depths along the boundaries of w, $\overline{w}$, and w' are identical except for possibly between boundary vertices i and $i+1$. Depths are integral, so in the first two cases the depth in $\overline{w}$ between i and $i+1$ must match that of w or w'.

In the third case, the depth between boundary vertices i and $i+1$ in $\overline{w}$ could be one greater than in w and one less than in w'. However, this would mean the Yamanouchi word for $\overline{w}$ would be identical to that of w and w' in all positions except positions i and $i+1$ where it would have symbols 00. This would lead to an unbalanced Yamanouchi word which is not possible. Hence we see in each of the three cases, if $w \preceq_S \overline{w} \preceq_S w'$ then $w = \overline{w}$ or $\overline{w} = w'$. We conclude the covering relation for $\prec_S$ contains the covering relation for $\prec_T$. □

Figure 20 exhibits $T, \widetilde{T} \in SYT(7,7,7)$ and their corresponding band diagrams on 21 boundary points. Using this data, we see the associated webs $\widetilde{w}$ and w have the property that $\widetilde{w} \prec_S w$ but $r(\widetilde{w}) > r(w)$. Hence, we obtain the following negative result relating $\prec_S$ and $\prec_T$.

Theorem 5.10. *The partial orders $\prec_S$ and $\prec_T$ on reduced $\mathfrak{sl}_3$ webs are different. In fact, $\prec_S$ is not ranked.*

6. Relating the Specht basis and $\mathfrak{sl}_3$ web basis

For $k \geq 2$, the space of $\mathfrak{sl}_k$ webs is equipped with an action of the symmetric group. Previous work by the authors and others focuses primarily on studying properties of the $\mathfrak{sl}_2$ instance of this action along with some preliminary investigation into the $\mathfrak{sl}_3$ case. The main motivation for studying band diagrams is to provide a useful combinatorial tool for characterizing the behavior of $\mathfrak{sl}_3$ webs under the action of the symmetric group. In particular, given $w \in \mathcal{W}_{3n}^R$ and simple transposition $s_i \in S_{3n}$, we wish to describe the reduced summands of $s_i \cdot w$. We begin this section with a description of the symmetric group action on $\mathfrak{sl}_2$ and $\mathfrak{sl}_3$ webs.

Given a simple transposition s_i and an $\mathfrak{sl}_2$ or $\mathfrak{sl}_3$ bottom web w, define $s_i \cdot w$ to be the sum of webs obtained by appending a crossing to the i and $(i+1)^{st}$ endpoints of w and smoothing according to Figure

$\widetilde{T} =$ 1 2 3 4 5 14 6 7 8 9 10 15 11 12 13 16 17 18	$T =$ 1 2 3 4 5 9 6 7 8 13 14 15 10 11 12 16 17 18
$\widetilde{B} =$ 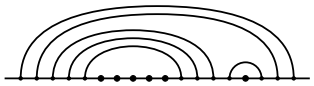	$B =$ 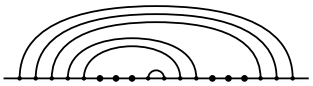
$S_1(\widetilde{w}) = [1, 21]$ $S_2(\widetilde{w}) = [2, 20]$ $S_3(\widetilde{w}) = ([3, 13] \cup [14, 19])$ $S_4(\widetilde{w}) = ([4, 12] \cup [15, 18])$ $S_5(\widetilde{w}) = [5, 11]$ $S_6(\widetilde{w}) = \emptyset$	$S_1(w) = [1, 21]$ $S_2(w) = [2, 20]$ $S_3(w) = [3, 19]$ $S_4(w) = [4, 12] \cup [15, 18]$ $S_5(w) = [5, 11]$ $S_6(w) = [9, 10]$
$r(\widetilde{w}) = 41$	$r(w) = 40$

FIGURE 20. Data for webs $\widetilde{w}$ and w with $\widetilde{w} \prec_S w$ and $r(\widetilde{w}) > r(w)$

FIGURE 21. Smoothing rules for symmetric group action on webs

21. (Note that his action comes from flattening a braiding on webs [**?**].) We consider $s_i \cdot w$ as an element of $\Gamma_{q=1}^{\mathcal{W}_{2n}}$ or $\Gamma_{q=1}^{\mathcal{W}_{3n}}$, and we can express it in terms of the reduced web basis by applying web reduction rules with $q = 1$. Figure 22 shows examples of the symmetric group acting on $\mathfrak{sl}_2$ and $\mathfrak{sl}_3$ webs.

In the $\mathfrak{sl}_2$ case, $s_i \cdot w$ has at most two summands. If i and $i+1$ are connected in w, then $s_i \cdot w = -w$. Otherwise, if i and $i+1$ are not connected in w, then w has arcs (i, j) and $(i+1, k)$ where these arcs could be nested or unnested. In this case, $s_i \cdot w = w + w'$ where w' is identical to w off of the vertices $i, i+1, j$, and k and w' has arcs (j, k) and $(i, i+1)$. This action on $\mathfrak{sl}_2$ webs leads to another description of the edges in the Hasse diagram for $\prec_T$. In particular, $w \xrightarrow{s_i} w'$ is an edge if and only if i is below $i+1$ in w and $s_i \cdot w = w + w'$. In the $\mathfrak{sl}_3$ case, the action of the symmetric group does not have an easy characterization. Given a simple transposition s_i and a reduced $\mathfrak{sl}_3$ web w, the quantity $s_i \cdot w$ can have an arbitrarily large number of reduced summands.

Recall that the complex, finite-dimensional representations of the symmetric group are parameterized by partitions. We have the following result which characterizes web space as a symmetric group representation. This is proven in [**?**, **?**] and we believe a more general result is also true as a consequence of Schur-Weyl duality, but we have not worked out the details.

Theorem 6.1. *The symmetric group representations $\Gamma_{q=1}^{\mathcal{W}_{2n}}$ and $\Gamma_{q=1}^{\mathcal{W}_{3n}}$ described above are irreducible and correspond to the partitions (n, n) and (n, n, n) respectively.*

Specht modules are a classic combinatorial construction of irreducible symmetric group representations. The (n, n) (resp. (n, n, n)) Specht module, which we will denote by $\Gamma^{\mathcal{T}_{2n}}$ (resp. $\Gamma^{\mathcal{T}_{3n}}$), has a basis indexed by $SYT(n, n)$ (resp. $SYT(n, n, n)$). Since the reduced web bases are also indexed by standard Young tableaux, it is natural to compare the Specht and web bases. In particular, we wish to describe the unique (up to scaling), nontrivial equivariant isomorphism ϕ between them.

Given a Young tableau T, we will write its corresponding Specht vector as v_T. We will not give a full description of the action of the symmetric group on the Specht basis. (An interested reader can find such an exposition in [**?**].) However, the following Specht module property is important in our discussion below.

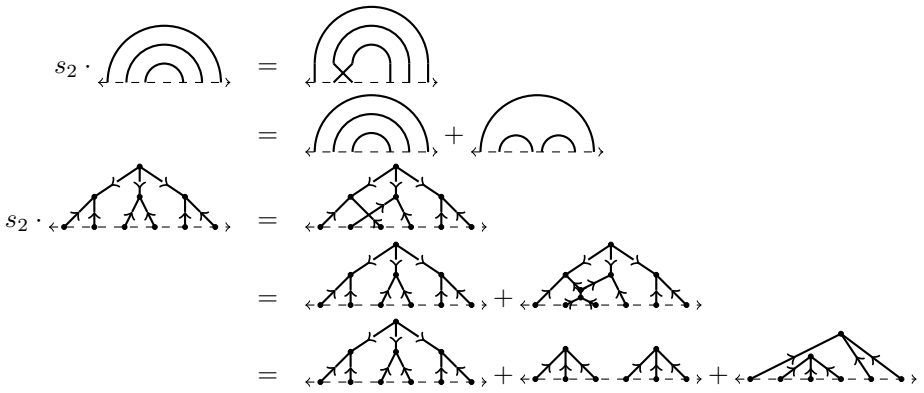

FIGURE 22. An example of the symmetric group action on $\mathfrak{sl}_2$ and $\mathfrak{sl}_3$ webs.

Proposition 6.2. *Let $T \xrightarrow{s_i} T'$ be an edge in the Hasse diagram for $\prec_T$. Then $s_i \cdot v_T = v_{T'}$.*

Remark 6.3. Note that in the $\mathfrak{sl}_2$ and $\mathfrak{sl}_3$ settings, the combinatorial bijection ψ^{-1} between tableaux and webs fails to extend to a map of representations. As a concrete example, consider the initial $\mathfrak{sl}_3$ web to which s_2 is applied in Figure 22. Call this web w. Observe that $\psi^{-1}\left(\begin{array}{|c|c|}\hline 1&3\\\hline 2&5\\\hline 4&6\\\hline\end{array}\right) = w$, and $s_2 \cdot T = T' = \begin{array}{|c|c|}\hline 1&2\\\hline 3&5\\\hline 4&6\\\hline\end{array}$. Now say $w' = \psi^{-1}(T')$. The calculation in Figure 22 shows that $s_2 \cdot w \neq w'$. In other words, ψ^{-1} is not equivariant since $s_2 \cdot \psi^{-1}(v_T) \neq \psi^{-1}(s_2 \cdot v_T)$.

The following result about the map ϕ in the $\mathfrak{sl}_2$ setting follows from Proposition 6.2 and the characterization of the symmetric group on $\mathfrak{sl}_2$ webs. It has recently been strengthened by Rhoades and ...

Theorem 6.4. *Let $<$ be any total order on $\mathcal{W}_{2n}^R$ that completes $\prec_T$ and respects rank, and let $\phi : \Gamma^{\mathcal{T}_{2n}} \to \Gamma_{q=1}^{\mathcal{W}_{2n}}$ be the unique (up to scaling) S_{2n}-equivariant isomorphism between the Specht and web modules. Using $<$ to order both the Specht and web bases, the matrix for ϕ is unitriangular with additional vanishing entries.*

The unitriangularity portion of Theorem 6.4 follows from an inductive argument and several lemmas characterizing the rank of reduced summands of $s_i \cdot w$. We would like to prove the same unitriangularity result in the $\mathfrak{sl}_3$ web setting. The approach to the $\mathfrak{sl}_2$ proof, however, does not entirely translate since the action of simple transpositions on $\mathfrak{sl}_3$ webs is much more complicated.

While it is difficult to analyze the rank of reduced summands of $s_i \cdot w$ in the $\mathfrak{sl}_3$ case, shadow containment is easier to track. Our current strategy for proving unitriangularity and the motivation behind this article has two parts. First, use band diagrams and shadows for $\mathfrak{sl}_3$ webs to describe the map ϕ between the Specht and $\mathfrak{sl}_3$ web modules. Then, use this information and the relationship between the partial orders $\prec_T$ and $\prec_S$ to prove a unitriangularity result analogous to Theorem 6.4.

The remainder of this paper is dedicated to (1) proving Theorem 6.11 which characterizes ϕ in terms of shadow containment and (2) providing insight into the interaction between $\prec_T$ and $\prec_S$. Lemma 6.5 is the base case for Theorem 6.11. Its proof is completely analogous to the $\mathfrak{sl}_2$ case, so we do not include it here [**?**].

Lemma 6.5. *Let $T_0 \in SYT(n,n,n)$ be the column-filled tableau, and let w_0 be the corresponding reduced web on $3n$ vertices. Then $\phi(v_{T_0}) = aw_0$ for some $a \neq 1$.*

For simplicity, assume $a = 1$ so that $\phi(v_{T_0}) = w_0$. The next three lemmas characterize shadows of reduced summands of $s_i \cdot w$ for all nine possible pairs of boundary symbols in the i and $(i+1)^{st}$ position of the boundary word for w. Proofs for these lemmas follow from straightforward case analyses.We give example calculations in Figure 23. See [**?**] for further examples of similar calculations.

Lemma 6.6. *If w has $+-$, $+0$, or $0-$ in the i and $(i+1)^{st}$ positions of its band word, then $s_i \cdot w = -w$.*

Lemma 6.7. *If w has $++$, 00, or $--$ in the i and $(i+1)^{st}$ positions of its band word, then $\widetilde{w} \prec_S w$ for all reduced summands $\widetilde{w} \neq w$ of $s_i \cdot w$.*

Lemma 6.8. *If w has $-+$, -0, or $0+$ in the i and $(i+1)^{st}$ positions of its band word, then $w \xrightarrow{s_i} w'$ is an edge in the Hasse diagram for $\prec_T$ and $\widetilde{w} \preceq_S w'$ for all reduced summands $\widetilde{w}$ of $s_i \cdot w$.*

Boundary word for w at i and $i+1$	**Local Calculation of $s_i \cdot w$ at vertices i and $i+1$**
$+-$	M-diagram for $w =$ 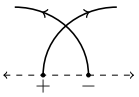 $w =$ 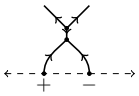 $s_i \cdot w = w + \widehat{w} =$  $= w - 2w$ **Conclusion**: In this case, $s_i \cdot w = -w$ as desired.
$++$	$w =$ 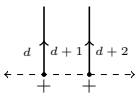 $s_i \cdot w = w + \widehat{w} =$ 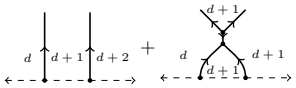 **Conclusion**: All reduced summands $\widetilde{w}$ of $\widehat{w}$ satisfy $\widetilde{w} \prec_S w$
00	M-diagram for $w =$ 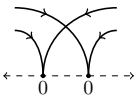 $w =$ 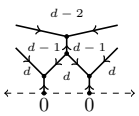 $s_i \cdot w = w + \widehat{w} =$ 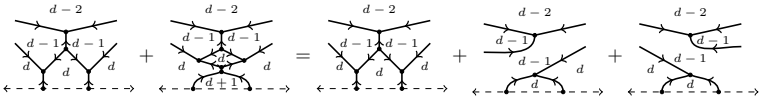 **Conclusion**: The web $\widehat{w}$ is always unreduced. All reduced summands $\widetilde{w}$ of $\widehat{w}$ satisfy $\widetilde{w} \prec_S w$.
-0	**Note**: In this case, $w \xrightarrow{s_i} w'$ is an edge in the Hasse diagram for $\prec_T$. $w =$ 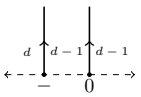 $w' =$ 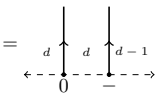 $s_i \cdot w = w + \widehat{w} =$ 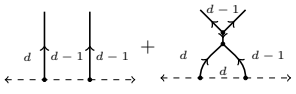 **Conclusion**: All reduced summands $\widetilde{w}$ of $\widehat{w}$ satisfy $\widetilde{w} \prec_S w'$

FIGURE 23. Case analysis examples for Lemmas 6.6, 6.7, and 6.8

In certain subcases of Lemma 6.8, we can prove a stronger result showing that $s_i \cdot w$ is a sum of webs in which w and w' each appear with coefficient 1 and all other reduced summands $\widetilde{w}$ satisfy $\widetilde{w} \prec_S w$. We suspect this is always true, but the following result is sufficient for our purposes and easier to prove.

Lemma 6.9. *Let w' be a reduced web with $r(w') > 0$, and consider the smallest i such that there exists an edge $w \xrightarrow{s_i} w'$ in the Hasse diagram for $\prec_T$. Then*

$$s_i \cdot w = w + w' + \sum_{\{\widetilde{w}:\widetilde{w} \prec_S w\}} \widetilde{c}\widetilde{w}$$

where $\widetilde{c} \in \mathbb{Z}$.

Proof. Let w and w' be as in the statement of the lemma. Then the boundary word for w up to and including the $(i+1)^{st}$ symbol has one of the following three forms:

- Case 1: $(+0-)^p(+0)^q(+)^r 0+$ where $p \geq 0$, $q \geq 0$, and $r \geq 1$
- Case 2: $(+0-)^p(+0)^q(+)^r -+$ where $p \geq 0$, $q \geq 1$, and $r \geq 0$
- Case 3: $(+0-)^p(+0)^q +-0$ where $p \geq 0$ and $q \geq 1$

To complete the proof, we sketch the relevant parts of the M-diagram for w, the web w, and $s_i \cdot w$ in each case. We indicate the i and $(i+1)^{st}$ endpoints in M-diagrams and webs with enlarged vertices.

First, consider a web w with boundary word as indicated in Case 1. The web and its M-diagram will have the following local structure.

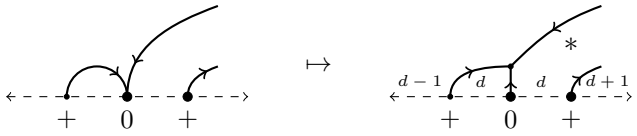

It is possible that M-diagram arcs incident to the i and $(i+1)^{st}$ boundary vertices exiting to the right could cross. If they do not cross, the starred region in w necessarily has more than 4 edges not including the boundary or touches the boundary elsewhere. If the arcs cross, then the starred region has exactly 4 edges not including the boundary.

Consider $s_i \cdot w = w + \widehat{w}$ when the arcs do not cross.

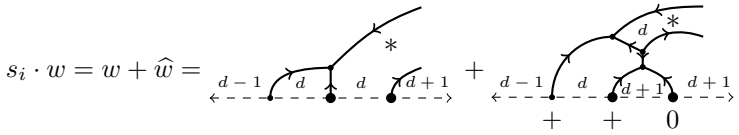

In this subcase, $\widehat{w}$ is reduced (since the starred region is not a square or bigon) and has a boundary word identical to w'. We conclude $\widehat{w} = w'$ and $s_i \cdot w = w + w'$. Next, consider the structure of web $\widehat{w}$ if the arcs incident to vertices i and $i+1$ do cross in the M-diagram for w. Then $\widehat{w}$ can be reduced as follows

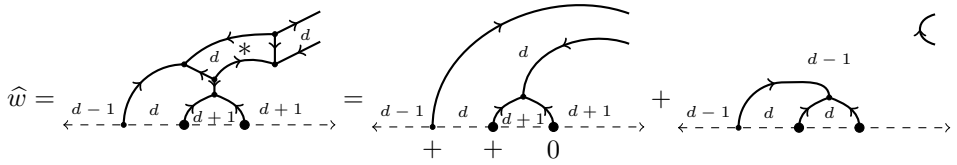

In this subcase, $\widehat{w}$ splits as the sum of a reduced (since no closed faces were created or modified) web whose boundary matches w' and a possibly unreduced web with region depths labeled as shown. Therefore, we have shown $s_i \cdot w = w + w' + \sum_{\{\widetilde{w}:\widetilde{w} \prec_S w\}} \widetilde{c}\widetilde{w}$ where $\widetilde{c} \in \mathbb{Z}$.

Now, consider a web w with boundary word as indicated in Case 2. The following is a local picture of both its M-diagram and the web itself.

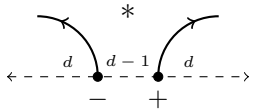

Since a third arc of the M-diagram for w cannot intersect both of the arcs shown, the starred region in this case will have more than 4 edges not counting the boundary or will touch the boundary elsewhere. Arguing as in the first subcase of Case 1 above, we can show $s_i \cdot w = w + \widehat{w}$ where $\widehat{w}$ is reduced and $\widehat{w} = w'$.

Finally, consider a web w with boundary word as indicated in Case 3. Local pictures of w and the M-diagram for w are as follows. Note that we expand the view of the M-diagram to show the starred region in w is not closed. This is an important observation in the next step.

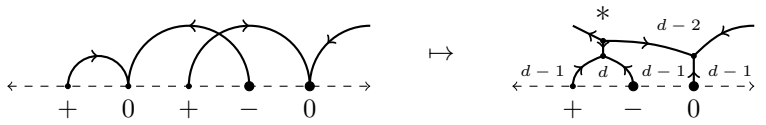

Acting on w by s_i, we will obtain $s_i \cdot w = w + \widehat{w}$ where $\widehat{w}$ reduces as shown below.

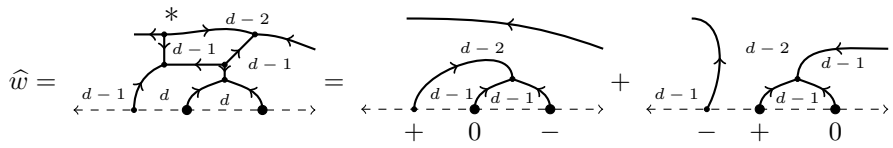

Since no regions adjacent to the square in $\widehat{w}$ are close, we see $\widehat{w}$ splits as the sum of two reduced webs one of which is w'. Hence, $s_i \cdot w = w + w' + \widetilde{w}$ where $\widetilde{w} \prec_S w$. □

The following lemma is key to the inductive proof of Theorem 6.11 below. Note that Lemmas 6.8, 6.9, and 6.10 already begin to give a sense of the interaction between the partial orders $\prec_S$ and $\prec_T$.

Lemma 6.10. *Let w, w', and $\overline{w}$ be reduced webs such that $\overline{w} \xrightarrow{s_i} w'$ is an edge in the Hasse diagram for $\prec_T$ and $w \prec_S \overline{w}$. Then for all reduced summands $\widetilde{w}$ of $s_i \cdot w$, it follows that $\widetilde{w} \prec_S w'$.*

Proof. First, note that $\overline{w} \xrightarrow{s_i} w'$ implies $\overline{w} \prec_T w'$, and by Lemma 5.9 it follows that $\overline{w} \prec_S w'$. Moreover, since $w \prec_S \overline{w}$ and $\overline{w} \prec_S w'$, we have $w \prec_S w'$. By Lemmas 6.6 and 6.7, we know if the boundary symbols for w in the i and $(i+1)^t$ positions are $+0, +-, 0-, ++, 00$, or $--$, then all reduced summands $\widetilde{w}$ of $s_i \cdot w$ satisfy $\widetilde{w} \preceq_S w$. Since $w \prec_S w'$, we conclude $\widetilde{w} \prec_S w'$ as desired in all of these cases.

For the remainder of the proof, assume the i and $(i+1)^{st}$ boundary symbols for w are $-+$, $0-$, or $0+$. Then Lemma 6.8 shows that there exists a reduced web w'' and an edge $w \xrightarrow{s_i} w''$ in the Hasse diagram for $\prec T$. From this same lemma, we know all reduced summands $\widetilde{w}$ of $s_i \cdot w$ satisfy $\widetilde{w} \preceq_S w''$, so it only remains to show $w'' \prec_S w'$.

Since the boundary words for w and w'' differ only at the i and $(i+1)^{st}$ symbols, the depths along the boundary of w and w'' differ only between vertices i and $i+1$. As we noted in the proof of Lemma 5.9, the depth between i and $i+1$ increases by 1 from w to w'' if the boundary word for w is $0+$ or -0 in the i and $(i+1)^{st}$ positions and increases by 2 if the boundary word is $-+$. The boundary depths in $\overline{w}$ and w' have the same relationship since there is also an edge $\overline{w} \xrightarrow{s_i} w'$.

We know $w \prec_S \overline{w}$, w and w'' have identical boundary depths except for between i and $i+1$, and $\overline{w}$ and w' have identical boundary depths except for between i and $i+1$. The only way it could occur that $w'' \not\prec_S w'$ is if the depths between i and $i+1$ are equal in w and $\overline{w}$ – let us call this common depth d – but the depth between i and $i+1$ is $d+2$ in w'' and $d+1$ in w'. We will show this can never happen.

If the depth between i and $i+1$ in w'' is $d+2$, then the boundary word for w at the i and $(i+1)^{st}$ positions is $-+$. It follows that the depths in w and w'' between $i-1$ and i as well as between $i+1$ and $i+2$ are $d+1$. Since $w \prec_S \overline{w}$, it follows that the depths in $\overline{w}$ between $i-1$ and i as well as between $i+1$ and $i+2$ are at least $d+1$. We assumed the depth between i and $i+1$ in $\overline{w}$ is d, so this would force the boundary word for $\overline{w}$ at the i and $(i+1)^{st}$ positions to be $-+$. However, this would imply the depth between i and $i+1$ in w' is $d+2$. Hence $w'' \prec_S w'$. □

Finally, we obtain the following theorem characterizing the coefficients of the transition matrix between the Specht and $\mathfrak{sl}_3$ web bases in terms of shadow containment.

Theorem 6.11. *Let $T' \in SYT(n,n,n)$ and w' be the reduced $\mathfrak{sl}_3$ web corresponding to T'. Then*

$$\phi(v_{T'}) = w' + \sum_{\widetilde{w} \in \mathcal{W}_{3n}^R} c_{\widetilde{w}}^{w'} \widetilde{w}$$

where $c_{\widetilde{w}}^{w'} = 0$ whenever $\widetilde{w} \not\prec_S w'$.

Proof. We will prove this theorem by induction on $r(T')$. If $r(T') = 0$, then $T' = T_0$. Lemma 6.5 shows $\phi(v_{T_0}) = w_0$, and the base case is proven.

Assume the theorem holds for all tableaux of rank k. Consider $T' \in SYT(n,n,n)$ such that $r(T') = k+1$. Choose the smallest value i such that there exists a reduced web w and an edge $w \xrightarrow{s_i} w'$ in the Hasse diagram for $\prec_T$, and let T be the tableau corresponding to w.

Then by Proposition 6.2, $s_i \cdot v_T = v_{T'}$. Since ϕ is equivariant, it follows that $\phi(v_{T'}) = \phi(s_i \cdot v_T) = s_i \cdot \phi(v_T)$. Since $r(T) = k$, we know by the inductive assumption that

$$\phi(v_{T'}) = s_i \cdot \phi(v_T) = s_i \cdot \left(w + \sum_{\widetilde{w} \in \mathcal{W}_{3n}^R} c_{\widetilde{w}}^{w} \widetilde{w} \right) = s_i \cdot w + \sum_{\widetilde{w} \in \mathcal{W}_{3n}^R} c_{\widetilde{w}}^{w} (s_i \cdot \widetilde{w})$$

where $c_{\widetilde{w}}^{w} = 0$ whenever $\widetilde{w} \not\prec_S w$.

First, consider $s_i \cdot w$. By Lemma 6.9, we know $s_i \cdot w = w + w' + \sum_{\{\widetilde{w} : \widetilde{w} \prec_S w\}} \widetilde{c}\widetilde{w}$ where $\widetilde{c} \in \mathbb{Z}$. Hence, w' occurs with a coefficient of 1 in $s_i \cdot w$ and all other reduced webs in $s_i \cdot w$ have shadows strictly contained in the shadow of w' as desired.

Now, let $\widetilde{w}$ be a reduced web such that $c_{\widetilde{w}}^{w} \neq 0$. Then $\widetilde{w} \prec_S w$. By Lemma 6.10, every reduced summand of $s_i \cdot \widetilde{w}$ has a shadow strictly contained in the shadow of w'. Hence $\phi(v_{T'})$ is a linear combination of reduced webs in which w' occurs with coefficient 1 and any other reduced web with a nonzero coefficient has shadow strictly contained in the shadow of w'. □

The following conjecture would upgrade Theorem 6.11 to the desired unitriangularity result.

Conjecture 6.12. *If $c_{\widetilde{w}}^{w'} \neq 0$, then $r(\widetilde{w}) < r(w')$.*

If $\widetilde{w} \prec_S w'$ implied $r(\widetilde{w}) < r(w')$, then Conjecture 6.12 would follow. Unfortunately, the example in Figure 20 shows this is not always the case. In order for Conjecture 6.12 to be true, however, it would be sufficient to show the shadow containment statements in Lemmas 6.7, 6.8, 6.9, and 6.10 can be replaced with rank inequalities. In particular, we make the following conjecture.

Conjecture 6.13. *Let $\widetilde{w}$ be a reduced summand of $s_i \cdot w$. Then $r(\widetilde{w}) \leq r(w) + 1$. Further, if $\widetilde{w} \preceq_S w$, then $r(\widetilde{w}) \leq r(w)$.*

The following result implies the webs $\widetilde{w}$ and w described in Figure 20 do not provide a counterexample to Conjecture 6.13. Recall that we denote the number of crossings in an M-diagram by $c(M)$.

Lemma 6.14. *Let $\widetilde{w}$ be a reduced summand of $s_i \cdot w$, and let $\widetilde{M}$ and M be the M-diagrams for $\widetilde{w}$ and w respectively. Then $c(\widetilde{M}) \leq c(w) + 1$. Moreover, $c(\widetilde{M}) = c(w) + 1$ if and only if $s_i \cdot w = w + \widetilde{w}$ and the boundary words for $\widetilde{w}$ and w differ as described in the following table.*

	Y-word for w	**Y-word for $\widetilde{w}$**	**Differ elsewhere?**
Case 1*:*	$0+$	$+0$	*No*
Case 2*:*	-0	$0-$	*No*
Case 3*:*	$-+$	$+-$	*No*
Case 4*:*	$++$	$+0$	*Yes*
Case 5*:*	$--$	$0-$	*Yes*

FIGURE 24. i^{th} and $(i+1)^{st}$ boundary symbols when $s_i \cdot w = w + \widetilde{w}$

Proof. Let $\widetilde{w}$, w, $\widetilde{M}$, and M be as in the statement of the lemma. To obtain a web from an M-diagram, each crossing is replaced with a pair of internal vertices - one source and one sink, and the middle of each M is replaced with a boundary edge and internal a sink vertex. This is illustrated in Figure 7. Hence the number of source vertices in a reduced web is the number of crossings in its M-diagram.

Given i, we compute $s_i \cdot w$ by appending a flattened crossing to the bottom of w at the i and $(i+1)^{st}$ vertices and resolving as a sum of webs as is shown in Figure 21. Say $s_i \cdot w = w + \widehat{w}$. The web $\widehat{w}$ is a possibly reducible web with one more source vertex than w. If $\widetilde{w} = w$, then $c(\widetilde{M}) = c(M)$ and we are done. Assume for the remainder of the argument that $\widetilde{w}$ is a reduced summand of $\widehat{w}$.

If $\widehat{w}$ is reducible, it either has a square or a bigon. If $\widehat{w}$ has a bigon, then boundary vertices i and $i+1$ were connected to the same internal vertex in w. Applying the bigon relation from Figure 2, it follows that $s_i \cdot w = w + \widehat{w} = w - 2w = -w$. If $\widehat{w}$ has a square, then expressing $\widehat{w}$ as a sum of reduced webs requires one or more applications of the square relation on $\mathfrak{sl}_3$ webs shown in Figure 2. Each application of this relation removes two source vertices, so a reduced summand of $\widehat{w}$ in these cases can have at most $c(M)$ source vertices, and we conclude $c(\widetilde{M}) \leq c(M)$.

If $\widehat{w}$ is reduced, then $\widehat{w} = \widetilde{w}$. A straightforward case analysis of the depths at i and $i+1$ under the action of s_i shows there are only five possibilities for the relationship between the boundary words of w and $\widetilde{w}$. These are shown in the table in Figure 24. In Case 1 - Case 3, the changes in depths are completely local. In Cases 4 and 5, the boundary word for $\widetilde{w}$ can only by balanced and Yamanouchi if it differs from the boundary word for w in at least one other position. □

Sketching the M-diagrams for webs $\widetilde{w}$ and w described in Figure 20, one can check that they have 10 and 9 crossings respectively. Examining their boundary words and comparing with the chart in Lemma 6.14, we conclude the following.

Corollary 6.15. *Consider the webs $\widetilde{w}$ and w with data shown in Figure 20. Given any i, $\widetilde{w}$ cannot be a summand of $s_i \cdot w$.*

While we can verify the example shown in Figure 20 does not yield a counterexample to Conjecture 6.13, we have not yet generalized this argument to a proof. Using the aid of a computer program, we have crossing, rank, and shadow data for all webs in $\mathcal{W}_{3n}^R$ with $n \leq 7$. Comparing the data for all pairs of webs, we have the following counts in Figure 25 which show the number of potential counterexamples in the $n = 6$ and $n = 7$ cases.

n	Count of $SYT(n,n,n)$	Number of pairs $\widetilde{w}, w \in SYT(n,n,n)$ such that $\widetilde{w} \prec_S w$ and $r(\widetilde{w}) > r(w)$	Number of these pairs with $c(\widetilde{M}) \leq c(M) + 1$
1	1	0	0
2	5	0	0
3	42	0	0
4	462	0	0
5	6006	0	0
6	87516	660	446
7	1385670	62147	40865

FIGURE 25. Number of possible counterexamples to Conjecture 6.13